Structural and Biophysical Analysis of Important Biomedical Enzymes and Nano-architectures

Inauguraldissertation
zur
Erlangung der Würde eines Doktors der Philosophie
vorgelegt der
Philosophisch-Naturwissenchaftlichen Fakultät
der Universität Basel

Von

Arundhati Chattopadhyay

Aus

Indien

Basel, 2009

Genehmigt von der Philosophisch-Naturwissenschaftichen Fakultät

Auf Antrag von

Professor. Dr. Ueli Aebi (University of Basel, Switzerland)

Und

Associate Professor. Dr. Peter Burkhard (University of Connecticut, USA)

Und

Professor. Dr. Tilman Schirmer (University of Basel, Switzerland)

Basel, den 14 Oktober 2008

Prof. Dr. Eberhard Parlow
(Dekan)

CONTENTS

Chapter 1

Structure, Mechanism, and Conformational Dynamics of *O*-Acetyl Serine Sulfhydrylase from *Salmonella typhimurium*: Comparison of A and B Isozymes†

(My contribution in this manuscript is the part that deals with crystallization and determination of the structure of OASSB enzyme).

Structure, Mechanism, and Conformational Dynamics of *O*-Acetylserine Sulfhydrylase from *Salmonella typhimurium*: Comparison of A and B Isozymes†

Arundhati Chattopadhyay,‡,§ Markus Meier,§ Sergei Ivaninskii,|| and Peter Burkhard*,§

Institute of Materials Science, University of Connecticut, 97 North Eagleville Road, Storrs, Connecticut 06269-3136, and M. E. Müller Institute for Structural Biology, Biozentrum, University of Basel, 4056 Basel, Switzerland

Francesca Speroni,‡ Barbara Campanini,* Stefano Bettati, and Andrea Mozzarelli

Department of Biochemistry and Molecular Biology, University of Parma, 43100 Parma, Italy

Wael M. Rabeh,‡ Lei Li,⊥ and Paul F. Cook*

Department of Chemistry and Biochemistry, University of Oklahoma, 620 Parrington Oval, Norman, Oklahoma 73019

Received December 19, 2006; Revised Manuscript Received April 2, 2007

ABSTRACT: *O*-Acetylserine sulfhydrylase is a pyridoxal 5′-phosphate-dependent enzyme that catalyzes the final step in the cysteine biosynthetic pathway in enteric bacteria and plants, the replacement of the β-acetoxy group of *O*-acetyl-L-serine by a thiol to give L-cysteine. Two isozymes are found in *Salmonella typhimurium*, with the A-isozyme expressed under aerobic and the B-isozyme expressed under anaerobic conditions. The structure of *O*-acetylserine sulfhydrylase B has been solved to 2.3 Å and exhibits overall a fold very similar to that of the A-isozyme. The main difference between the two isozymes is the more hydrophilic active site of the B-isozyme with two ionizable residues, C280 and D281, replacing the neutral residues S300 and P299, respectively, in the A-isozyme. D281 is above the *re* face of the cofactor and is within hydrogen-bonding distance to Y286, while C280 is located about 3.4 Å from the pyridine nitrogen (N1) of the internal Schiff base. The B-isozyme has a turnover number (V/E_t) 12.5-fold higher than the A-isozyme and an ∼10-fold lower K_m for *O*-acetyl-L-serine. Studies of the first half-reaction by rapid-scanning stopped-flow indicate a first-order conversion of the internal Schiff base to the α-aminoacrylate intermediate at any concentration of *O*-acetyl-L-serine. The K_d values for formation of the external Schiff base with cysteine and serine, obtained by spectral titration, are pH dependent and exhibit a pK_a of 7.0−7.5 (for a group that must be unprotonated for optimum binding) with values, above pH 8.0, of about 3.0 and 30.0 mM, respectively. In both cases the neutral enolimine is favored at high pH. Failure to observe the pK_a for the α-amines of cysteine and serine in the pK_{ESB} vs pH profile suggests a compensatory effect resulting from titration of a group on the enzyme with a pK_a in the vicinity of the α-amine's pK_a. The pH dependence of the first-order rate constant for decay of the α-aminoacrylate intermediate to give pyruvate and ammonia gives a pK_a of about 9 for the active site lysine (K41), a pH unit higher than that of the A-isozyme. The difference in pH dependence of the pK_{ESB} for cysteine and serine, the higher pK_a for K41, and the preference for the neutral species at high pH compared to the A-isozyme can be explained by titration of C280 to give the thiolate. Subtle conformational differences between *O*-acetylserine sulfhydrylase A and *O*-acetylserine sulfhydrylase B are detected by comparing the absorption and emission spectra of the internal aldimine in the absence and presence of the product acetate and of the external aldimine with L-serine. The two isozymes show a different equilibrium distribution of the enolimine and ketoenamine tautomers, likely as a result of a more polar active site for *O*-acetylserine sulfhydrylase B. The distribution of cofactor tautomers is dramatically affected by the ligation state of the enzyme. In the presence of acetate, which occupies the α-carboxylate subsite, the equilibrium between tautomers is shifted toward the ketoenamine tautomer, as a result of a conformational change affecting the structure of the active site. This finding, in agreement with structural data, suggests for the *O*-acetylserine sulfhydrylase B-isozyme a higher degree of conformational flexibility linked to catalysis.

O-Acetylserine sulfhydrylase (OASS)[1] catalyzes the final reaction of the cysteine biosynthetic pathway in bacteria and plants, the conversion of *O*-acetyl-L-serine (OAS) and bisulfide to L-cysteine and acetate (*1*). In enteric bacteria there are two isozymes of OASS, A and B. The B-isozyme of *O*-acetylserine sulfhydrylase (OASS-B) is expressed in

† This work was supported by the Grayce B. Kerr endowment to the University of Oklahoma to support the research of P.F.C., the Swiss National Science Foundation and the M. E. Mueller Foundation (to P.B.), and grants from the Italian Ministry of University and Research (COFIN2005 to A.M.) and the International Exchange Program 2005 (to A.M. and P.F.C.). The Istituto Nazionale di Biostrutture e Biosistemi is gratefully acknowledged.

* Corresponding authors. P.F.C.: tel, 405-325-4581; fax, 405-325-7182; e-mail, pcook@ou.edu. P.B.: tel, 860-486-3830; fax, 860-486-4745; e-mail, Peter.Burkhard@uconn.edu. B.C.: tel, 39-0521906613; fax, 39-0521905151; e-mail, barbara.campanini@unipr.it.

‡ These authors contributed equally to the work.

§ University of Connecticut.

|| University of Basel.

⊥ Current address: Department of Biochemistry, Albert Einstein College of Medicine, 1300 Morris Park Ave., Bronx, NY 10461-1602.

10.1021/bi602603c CCC: $37.00
Published on Web 06/21/2007

Chapter 2

Purification and Characterization of human DOPA-decarboxylase

2.1 Abstract

Dopa decarboxylase (DDC) is an important enzyme in the catecholamine biosynthesis pathways. Catecholamines, e.g., dopamine, serotonin, etc. often are the major neuromodulators or neurotransmitters. Hence, DDC plays a key role in regulation of neurodegenerative diseases like Parkinson's disease (PD). In order to achieve a medicine for PD, a successful inhibitor for DDC, that could reduce the activity of DDC in the blood while making it more effective in brain, is required. An effective design of an inhibitor requires a detailed structural study of human DDC. It was aimed to solve the DDC structure by X-ray crystallography. In order to have enough protein the DDC encoding gene has been cloned in the pET21d vector which was later termed as pET-DDC-His. However, it required numerous trials and errors until a suitable condition for soluble DDC expression was found. Addition of additives like PLP, ethanol, a complex of sorbitol and betaine in the growth medium of the bacteria did not help bring the protein in the soluble part as it formed inclusion bodies. Several soluble protein fusions with DDC, like Thioredoxin and Glutathione-S-transferase were also not quite helpful towards achieving soluble expression of DDC. Finally, a coexpression of DDC along with bacterial chaperone proteins, e.g., GroEL and GroES (after cotransforming both the DDC and Chaperone protein encoding plasmid in the same *E.coli* cell, used for expression) lead to solubilization of recombinant human DDC. This enzyme was then purified to homogeneity by successively passing the crude bacterial proteins through Ni-chelate-affinity chromatography and Size Exclusion Chromatography. The purified protein (>90 % purity) did not produce a good yield (4mg/ 8L culture), but this was enough to start the initial crystallization trial. Using a scale up to a 50 L culture, quite a good amount of protein was achieved. The homogeneity of DDC was further confirmed by using Multi-Angle Light Scattering and Blue Native PAGE. The dimeric enzyme preparation was then utilized for crystallization using the Hanging Drop Vapor Diffusion method. In a particular condition of the crystal screens trigonal bipyramidal crystals formed. However, these crystals did not show good diffraction when bombarded with X-ray beams. Later, this particular crystallization condition remained irreproducible.

2.2 Introduction

2.2.1. The Enzyme DOPA Decarboxylase

DOPA decarboxylase (DDC) or so called amino acid decarboxylase (AADC), is the enzyme involved in the synthesis of the catecholamine neurotransmitters, dopamine and serotonin. Tyrosine hydroxylase, another enzyme in this metabolic pathway, catalyzes the hydroxylation of a tyrosine residue to produce L-dihydroxyphenyl alanine (L-DOPA), which is eventually decarboxylated by DDC to form dopamine (Figure 2.1). Dopamine is particularly abundant in brain and basal ganglia and is the precursor of the catechol family of hormones viz. epinephrin and norepinephrin. A similar sequence of reactions in nervous system produce 5-OH tryptophan in the presence of tryptophan hydroxylase, decarboxylation of which by DDC produces serotonin.

DDC is a homodimeric pyridoxal phosphate (PLP) dependent enzyme[4]. Ichinose *et.al*.[5] prepared a cDNA clone after screening the human pherocytochroma cDNA library with a oligoneucleotide probe corresponding to the partial amino acid sequence purified from a tumor. The cDNA clone encoding 485 amino acids possesses a molecular mass of 53.8 kD[6]. The conserved amino acid sequence, Asn-Phe-Asn-Pro-His-Lys-Trp, in human, drosophila, and pig enzymes, has been found to be responsible for a possible pyridoxal phosphate cofactor-binding[7]. The protein encoded by hepatoma cells is the same as that encoded by adrenal chromaffin-derived pheochromocytoma cells.

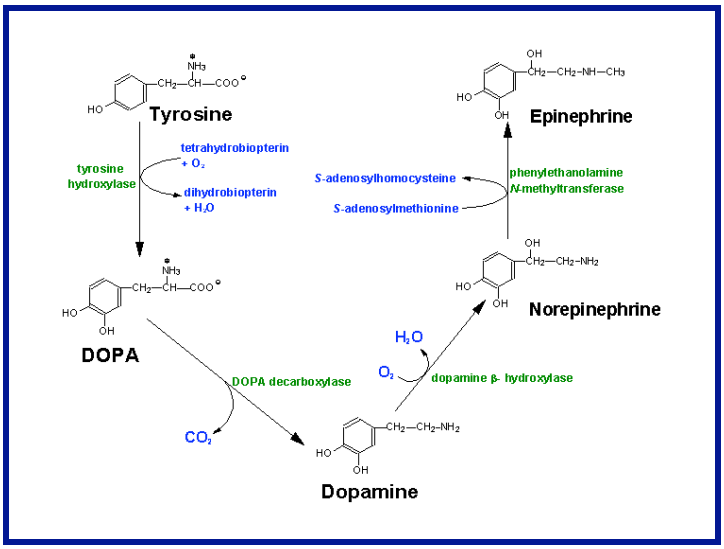

Figure2.1: Dopamine synthesis pathway. The role of DOPA decarboxylase in catecholamine (neurotransmitter) biosynthetic pathway. The picture was collected from web.indstate.edu/

2.2.2. Physiological Importance and Regulation of DDC

The primary function of DDC in the midbrain is the neurotransmission through monoaminergic neurons by involving itself in the synthesis of neuromodulators. Thus, DDC actually plays a major role in voluntary movement regulation[8]. Dopamine, physiologically the most important neurotransmitter in the *substantia niagra*, gets projected through the dopaminergic neurons and hence, these nurons are the major source of dopamine. However, a significant depletion of dopamine level is associated with the gradual loss of the number of dopaminergic nerve cells[9] that in turn causes poor stimulation of motor-nerves in this mechanistic cascade. Hence, degenerating dopaminegic neurons is the origin of motor-dysfuntion, which is manifested in the Parkinson's Disease syndrome.

2.2.3. Clinical Relevance of DDC

2.2.3.1. Parkinson's Disease and it's Treatment

Parkinson's disease (PD) is a chronic and progressive neurodegenerative disorder most commonly characterized by tremor, rigidity, postural-instability, slow movement (bradykinsia) and in extreme cases loss of physical movement (akinsia). The motor malfunction is associated with a lower level of stimulation of motor neurons by the dopamine depleted impaired dopaminergic neurons[10].

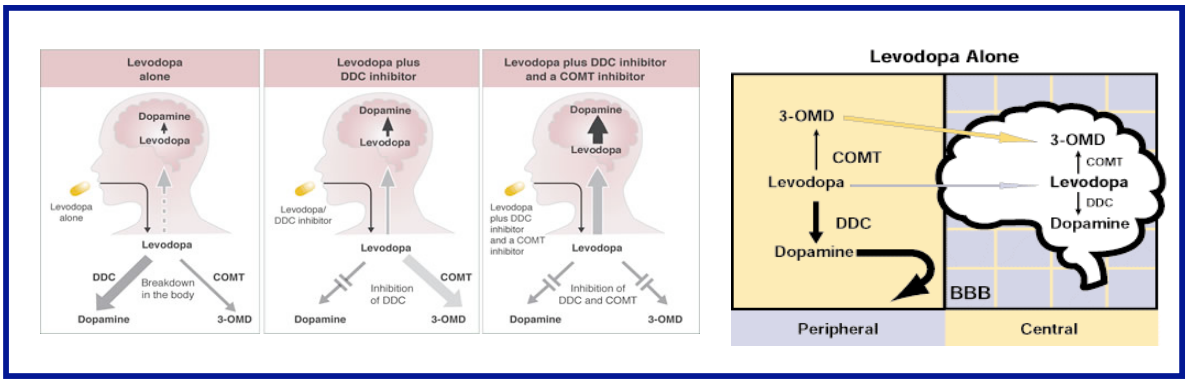

Figure2.2: Regulation of the production of dopamine in blood and brain. The picture was collected from http://www.epda.eu.com

PD symptoms are revealed when the level of dopamine in the basal ganglia of the brain is abnormally low. When dopamine synthesis deteriorates, the dopaminergic neurons start disappearing. Hence, restoring dopamine level back to normal is one of the ways of treating PD. However, dopamine cannot be directly administered in the blood as this compound cannot pass the Blood-Brain Barrier (BBB) to reach the brain. For this reason, L-DOPA, the precursor of dopamine, which can penetrate the BBB, is used for the treatment.

The L-DOPA treatment however, had encountered serious side effects like nausea, vomiting, blood pressure changes and collapse[11]. This is because, L-DOPA is also a component of other peripheral organs like the liver, kidney etc[12]. An elevated level of dopamine disturbs the chemical balances in these organs. Therefore, the use of the inhibitors, which selectively compete for dopamine production with the rate-limiting enzyme DDC in peripheral organs, has been recommended to use simultaneously during L-DOPA application[13]. Such an inhibitor-aided system would help increase the level of dopamine in the brain. A few competitive inhibitors of DDC have been depicted in the Figure 2.3 which structurally resemble L-DOPA, e.g., carbiDOPA[14], benserazide[15] etc. Therefore, the recent research effort mainly focuses on the reduction of L-DOPA dose and lowering of the side effects.

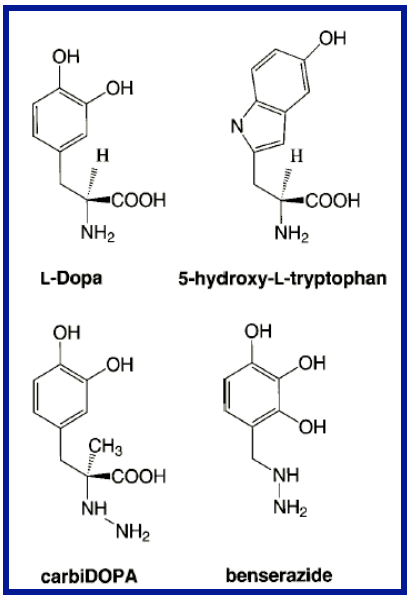

Figure 2.3. The chemical structures of DDC substrates and inhibitors. The substrate L-DOPA and 5 hydroxy-tryptophan together with the inhibitors carbiDOPA and benserazide (in its cleaved form) of DDC (Picture is taken from Burkhard et. al 2001).

2.2.3.2. Schizophrenia

The involvement of dopamine and dopaminergic pathways in the disease onset of schizophrenia has been confirmed [16]. A multifold decrease in the dopamine level

is observed in the sub-cortical region of brain leading to lesions in these areas [17]. This type of partial seizure in the brain is responsible for the psychosis as seen in the Schizophrenics. These patients with partial seizures evidenced to have significant increase in the DDC activity. Apart from dopamine, presence of a few other neurotransmitters/ neuromodulators is also indicative of the diseased condition, e.g., 2-phenylethylamine (2-PE) [16],[18],[19]. DDC, also known as aromatic L-amino acid decarboxylase (AADC), takes part as rate limiting enzyme in the production of the trace amines, namely, 2-phenylethylamine (2-PE), *p*-tyramine, and tryptamine which are thought to act as neuromodulators.

All of these above mentioned facts/evidences point out towards the importance of DDC being an interesting candidate enzyme for its susceptibility to schizophrenia. The data of structure -function of DDC is therefore of high demand in the development of therapeutic agents for Schrizophrenia.

2.2.3.3. Cancer

A number of peripheral cancers, namely, pheochoromocytomas are characterized by an extremely high DDC activity[20]. The significance of this strong catecholamine expression is not readily understandable. Analysis of the amount of expressed mRNA shows that the catecholamine production in pheochromocytomas is primarily controlled by the level of gene expression [21]. The large increase in DDC activity in cancerous cells can be important for chemotherapy. Hence, DDC is a candidate, against which the enzyme activated cytotoxic agents can be directed[22].

2.2.4. DOPA Decarboxylase - A member of PLP Dependent Enzyme

2.2.4.1. What is PLP?

Chemically, the compound, PLP, is termed as pyridoxal phosphate. It is a remarkably versatile coenzyme, categorized in the class of vitamin-B6. Vitamin-B6 enzymes are often involved in decarboxylation, racemization, transamination and many such reactions related to the modification of amino acid side chains. Three different chemical forms of vitaminB6 are mostly available *in vivo*. PLP is the predominant one, while the others are pyridoxine and pyridoxamine 5'-phosphate (PMP) (Figure 2.4).

2.2.4.2. PLP is One of Nature's Most Versatile Catalysts

PLP-dependent enzymes (B6 enzymes) catalyze a wider variety of different reactions than those containing any other cofactor. The common features of PLP catalysis underlying these diverse reactions are[23]:

1) PLP starts to be attached covalently by a Schiff's base linkage to a lysine residue located at the active site, giving what is called the "internal aldimine" form of the enzyme.

2) Upon binding an amino acid substrate, a transaldimination reaction releases the lysine residue and forms an "external aldimine" (PLP is held in place by only non-covalent interactions) between the substrate and PLP.

3) Finally, the amino acid substrate is hydrolyzed.

The PLP molecule in the Schiff base conformation provides an alternating double bond system that helps labializing free electrons and thus stabilizing it[24]. At this point, the conjugated orbital system in PLP effectively acts as a temporary electron storage site ('electron sink'), allowing several possible reactions to take place (Figure 2.5). The strong electron withdrawing system thus helps weaken the sigma bond of the α-carbon of the attached amino acid. This way, this particular carbon atom becomes an active reaction center on which elimination, substitution etc. processes can happen further. The geometry of PLP with respect to the enzyme, is in such a way established that an energy minimization is achieved by a sigma-pi interaction[25].

This common mechanism of initial internal and external aldimine complex formation guides the further specific reaction path depending on the ionic environment provided by the enzyme part, geometry of the intermediate, and/or presence of a metal ion[26]. Hence, the ring stabilization of PLP is the key to the versatility in action of this cofactor.

Despite the low sequence identity, the structural features of the different proteins are conserved amongst the common ancestors (Lesk and chothia 1980). Depending on the independent evolutionary lineages [27] the PLP dependent enzymes also have been categorized into five distinct structural groups ([28]). The so-called fold-type I is the most common structure, and is seen mostly in the aminotransferase and decarboxylase enzymes that catalyse α-,β or γ-eliminations[29]. Majority of the fold-type II group of enzymes catalyse β-elimination reactions[30]. Fold-type III, is characterized by a (β/α)8 barrel structure (prominent in alanine racemase and in a few types of amino-acid decarboxylases)[30]. Fold type IV mostly constitute the D-amino acid superfamily of the enzymes. Finally, the fold-type V group includes glycogen phosphorylase family of the PLP dependent enzymes[30]. This type of limited structural diversity is mostly attributed to the common basic mode of reaction that takes place because of the presence of PLP in the enzymes.

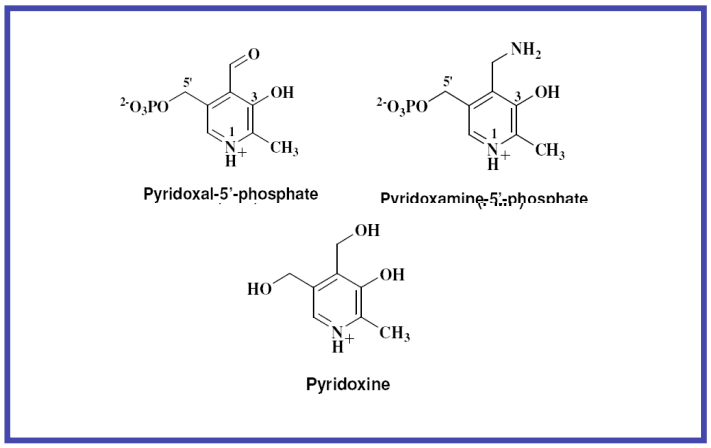

Figure2.4: The three forms of vitamin-B6

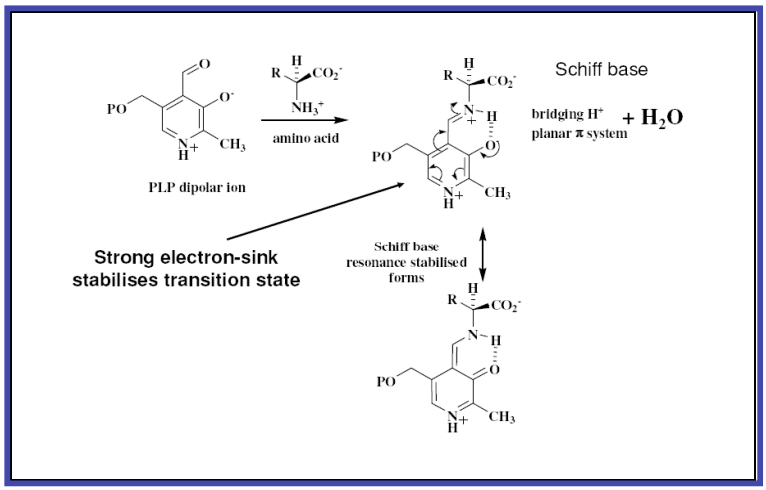

Figure2.5: Formation of Electron sink in PLP. The schematic of stabilization of PLP dependent enzymes by PLP during nucleophilic attack of the substrate.

2.2.4.3 Ketoenamine and Enolenamine Tautomeric Equilibrium

The tautomeric equilibria between the two forms of Schiff Base viz. enolimine and ketoenamine forms, is responsible for showing up two additional peaks at ~335 nm and ~420 nm in all of the PLP dependent enzymes apart from the one at 280 nm (Figure 2.6). The peak at ~ 420 nm indicates a protonated Schiff base linkage between the aldehyde group of PLP to the ε-NH_2 group of the representative Lys residue from the enzyme (e.g. Lys-303 in the case of pig DDC) indicative of the

ketoenamine form of the internal Schiff base (ISB) (Figure 2.6, 2 and 3). The absorbance at around 330 nm is due to the enolimine form (Figure 2.6, 1).

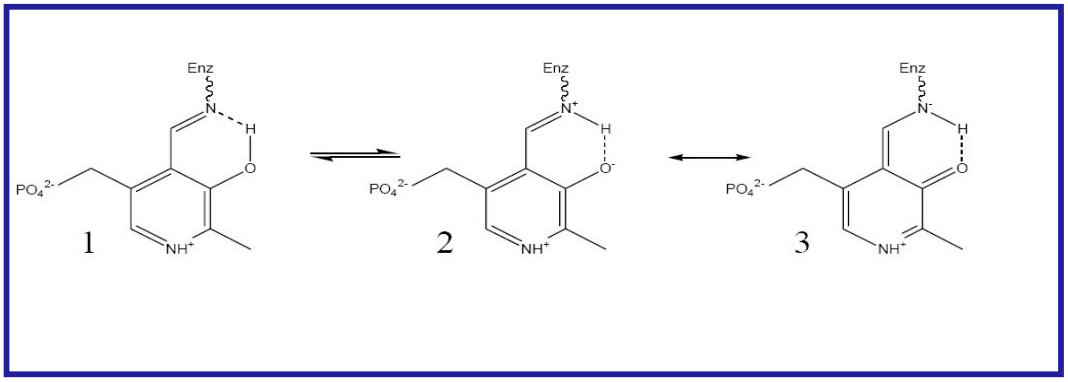

Figure2.6: Tautomeric and resonance forms of the internal aldimine.
1) Enolimine structure; 2 and 3) ketoenamine resonance forms.

Formation of the external Schiff base (ESB) slightly distorts the conenzyme plane, i.e., a Met adduct of the enzyme OASS causes 13° tilt of the PLP plane compared to that in ISB[31]. This change in geometry is also reflected in the change of λ_{max} ketoenamine and enolimine form, depending on the environment provided by the enzyme.

2.2.5. Structure of Pig-kidney DDC - A Clue to the Structure of Human DDC?

2.2.5.1. Structure of pig-kidney DDC

Burkhard *et al*. (2001) [3]describe the three-dimensional X-ray crystal structure of the pig-kidney DDC in the ligand-free form and in complex with the anti-Parkinson drug carbiDOPA. DDC possesses an α2-dimeric structure - a typical fold of the α-family of PLP-dependent enzymes. Each of the two monomers in a molecule is composed of three distinct domains viz. a large domain, a small domain and an N-terminal domain (Figure 2.7). One PLP per subunit is bound deep inside the large domain. Eight alpha helices encompassing central seven-stranded beta sheet in the α-β fold make up the large domain. The small domain consists of a four-stranded antiparallel beta sheet with three helices residing opposite to the large domain. The N-terminal domain forms a cap like structure that flaps over the top of the other subunit. This domain consists of two parallel helices joined to an extended strand. The first helix of one subunit aligns antiparallel to the equivalent helix of the other subunit. Residues 75-77 (N-terminal domain) and residues 433-435 (small domain) form a short two-stranded β-sheet.

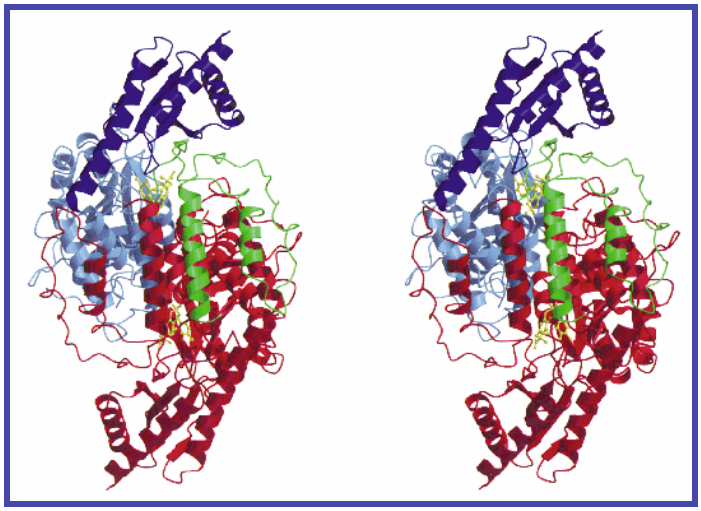

Figure2.7: Stereo view ribbon diagram of the polypeptide backbone of DDC. The view is directly down the two-fold symmetry axis. One monomer is completely red, whereas the other is green (N-terminal domain), cyan (large domain) and blue (small domain). The cofactors (PLP) and the inhibitors (carbiDOPA) are shown in ball-and-stick representation in yellow. The N-terminal domain of one monomer packs on top of the other monomer, resulting in an extended dimer interface. This picture was taken from Burkhard. *et. al.* (2001)[3]

2.2.5.2. Active Site

The active site of pig-kidney DDC, as explained by Burkhard *et al*.[3], constitutes mainly the residues from a single monomer even though, it is located near the interface of two monomers. In absence of the substrate or ligand, Lys-303 forms a Schiff base linkage with the aldehyde group of the PLP molecule. In the ligand free form, the carboxyate group of the Asp-271, situated in close proximity to the PLP, forms a salt-bridge with the protonated pyridine nitrogen, thus producing a strong electron sink stabilizing the carbanionic intermediate and facilitating the decarboxylation reaction. The phosphate group of the cofactor is further connected to the protein through an extended hydrogen bond network with the residues like Gly and Thr from a helix of the large domain. The residual positive charge of this end of the helix dipole neutralizes the negative charge of the phosphate moiety. In an experiment previously carried out by Dominici *et al* [32], an Ala residue replaced the Cys-111 or the formation of a disulfide bridge abolishes enzyme activity[3]. This is because the sulfhydryl group of Cys 100' is only 4.1 A apart from that of Cys-111. A mobile loop similar to the 'movable domain' of β-family enzyme (as discussed in the case of OASSA and B in chapter1) was found to be missing in the recombiant DDC crystal structure. Seemingly, these 11 residues (328-339) are important for catalysis and probably occlude in the active site cleft during the catalytic reaction.

2.2.5.3. Inhibitor Binding Mechanism

The form of DDC inhibitor carbiDOPA bound mimicks external aldimine structure of the enzyme-substrate complex. CarbiDOPA, which structurally resembles the substrate L-DOPA (Figure 2.3, Page 28), binds PLP by forming a hydrazone linkage through its hydrazine moiety. The catechol ring of carbiDOPA is implanted deep inside the active site cavity. Thr-82 of the enzyme, located near the phosphate group of PLP, is bound to the 4'-catechol hydroxyl group of the inhibitor (Figure 2.8). His-192, a highly conserved residue in almost all the α-family PLP enzymes, is placed in the front of the active site stacking its imidazole ring plane in parallel over the pyridine ring (Figure 2.8). The imidazole ring of His-192 possibly could play an important role in catalytic activity, because H192A mutants lose catalytic activity completely. Burkhard *et al* (2001)[3] hypothesize that His-192 catalytically activates the side chain of Tyr-332. In the active site Lys-303 displaces the amino group of the product through a nucleophilic attack on the imine bond resulting in releasing of the product. The reaction is controlled by the specificity of PLP-dependent enzymes, in which the external aldimine intermediate orients itself perpendicularly to the coenzyme π-bonding system (Figure 2.8). Therefore, the reaction is optimized, because the s-p orbital overlap in the transition state is maximized. Upon close examination of the complex, the carboxylate moiety of the inhibitor is oriented with the C_α-CO_2- bond approximately orthogonal to the plane of the coenzyme ring. This particular orientation is advantageous to achieve stereoelectric effects directing the specificity of the reaction.

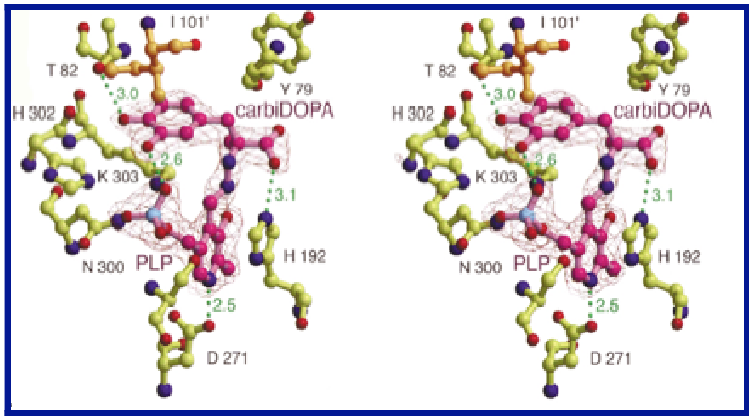

Figure2.8: A stereo diagram of the active site of inhibitor (carbiDOPA) bound DDC. The covalent linkage of carbiDOPA with Thr82 and the PLP N is shown in this picture. (This picture is taken from Burkhard *et al*, 2001).

2.2.5.4. Sequence Homology of Pig-kidney DDC and Human DDC

A sequence alignment result shows 87% sequence homology between pig-kidney and human DDC enzymes (Figure 2.9). The active site residues important for catalysis viz. Lys-303, His-302, His-192, Thr-82, Asp-271 (Figure 2.9.) are unchanged in both the homologues. There is a minor change with the similar type of amino acid (replacement of Lys-431 with Arg-431) at the C-terminus of the sequence that is near the domain that is responsible for making a two stranded β-sheet with the N-terminus part of the sequence. The remarkable change in the DDC is only limited to a region of two successive amino acids of human DDC viz. Asn-134 and Glu-135 which replace Ala-134 and Gly-135 in the pig-kidney enzyme. Another region, which has an interesting difference, is the residue just prior to the conserved Tyr-332. While in the pig-kidney DDC there is a hydrophobic residue adjacent to this amino acid, in human DDC the residue is replaced by a hydrophilic Thr-331 residue (Figure 2.9). All these changes in the sequence could help in modeling the human DDC structure and possibly could throw light on the approximate interaction that possibly could take place. But, the best way to understand the effect of these changes in residues or to explain the differences in solution behavior of these two enzymes, the structure of human DDC needs to be solved.

2.2.5.5. Structure Based Drug Design

Structure based drug designing is an improved technique over the traditional drug library screening. Such a designing process relies on the availability of the active site/regulatory domain cleft conformation of the disease related protein/enzyme target so that a small organic molecule, whose binding specificity to the very cleft resembles that of the natural substrate, could be synthesized *in-vitro*. The binding site structure, which eventually works as a mould to generate a precise ‘lead’ in drug discovery considering the three dimenstional steric, hydrophobic and hydrogen-bond interactions, could be best gathered by the X-ray crystallographic technique.

As described before, the high demand for effective PD treatment necessitates discovery of a potent inhibitor for DOPA decarboxylase in order to stop this enzyme action in blood, converting L-DOPA to dopamine. Despite the fact, the pig kidney DDC structure is now known, many other mechanistic questions related to inhibitor and human DDC interaction remains. The crystal structure of human DDC would assist in providing a stronger platform in developing more potent DDC inhibitors than the ones that have been used recently. The new drugs with the improved pharmacological character might allow for reduction of dosage of L-DOPA and hence could reduce very undesirable side effects.

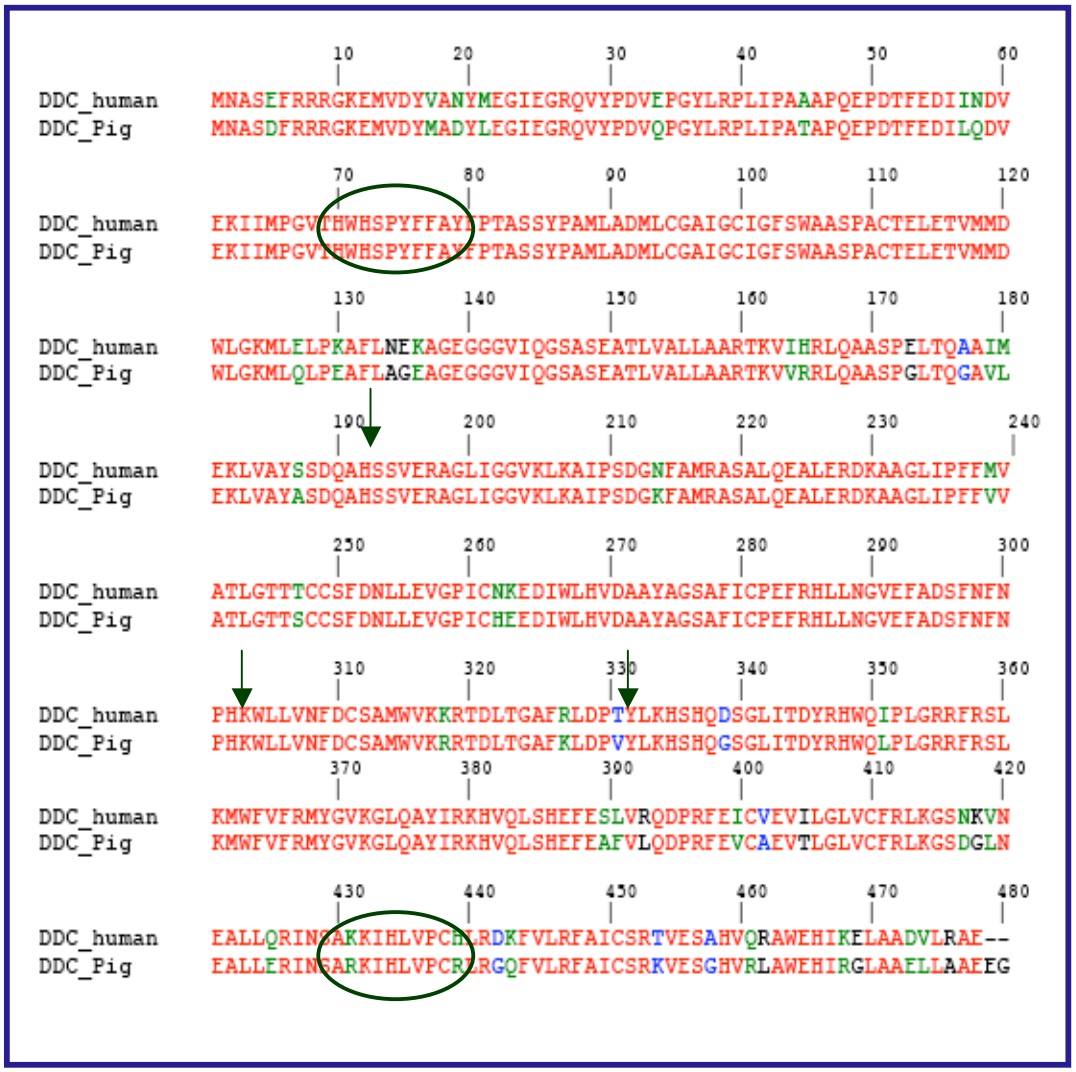

Figure 2.9: Sequence alignment of human- DDC and pig kidney- DDC showing 87% homology. Green oval marked area in the sequence are those which are stabilized by making an inter-domain β-sheet formation. The green arrowed amino acids represent the most conserved and catalytically active amino acids. Alignment was done using ClustalW, PBIL.

2.3 Scope of The Work

The scope of this thesis work includes purification, characterization and determination of the structure of Human DDC. X-ray crystallography was intended to be used in order to solve the structure of DDC.

Chapter 3

De-novo designed nanoparticles - an efficient pharmacological tool

3.1. Abstract

The peptide nanoparticle, designed and produced in our lab, could possibly be a very valuable tool in biomedical applications, e.g., in designing vaccines, delivering drugs, bioimaging, serodiagnosis, etc. The design of the peptide nanoparticles is based on the application of the symmetry elements of virus icosahedral capsid on a specially designed building block peptide. The designed peptide building block contains two oligomerization motifs, i.e., a trimeric coiled coil and a pentameric coiled coil joined by a linker region. Sixty such peptide units, upon self-assembly, would produce peptide nanoparticle mimicking a small icosahedral virus particle. The peptide chains in the building block provide flexibility in the design so that an additional peptide could be attached to it at the C-terminus in order to functionalize the peptide nanoparticle for various biomedical applications.

First of all, the functional peptide at the C-terminus could be an epitope for the antibody of a life threatening disease like HIV. These peptide nanoparticles can then function as the potent vaccine candidate for that particular disease. In this thesis work, I have attached the two epitopes against the two broadly neutralizing classes of antibody for HIV infection, 2F5 and 4E10, to the peptide nanoparticle.

Secondly, another sequence of peptide, which proved to have the capacity of seeding gold on its surface, was attached to the building block peptide unit. The nanoparticle, functionalized with such a peptide, can decorate a gold layer surrounding it. Gold coating on the peptide nanoparticle scaffold can provide a nanostructure, called 'nanoshells', which could be very important in the field of therapeutics because of its ability in easy detection and quick treatment of cancer cells.

Lastly, I added three peptides; those are recognized in the culture filtrates of *M.tuberculosis* isolated from TB patients, separately, to the basic peptide construct to form three different nanoparticles. Also, I tried to make a single nanoparticle that displays all the three peptides on its surface. Such a nanoparticle could be a very useful tool in the serodiagnosis or the antibody-based rapid detection of the deadly disease- Tuberculosis.

The nanoparticle formation in each of the above-mentioned cases was more or less successful. One of the constructs could successfully even produce gold shells on the peptide nanoparticle.

3.1 Introduction

3.1.1. Nanoparticles

"There is no accepted international definition of a **nanoparticle**, but one given in the new PAS71 document developed in the UK is: "A particle having one or more dimensions of the order of 100 nm or less".
There is a note associated with this definition: "Novel properties that differentiate **nanoparticles** from the **bulk material** typically develop at a critical length scale of under 100 nm".
The "novel properties" mentioned are entirely dependent on the fact that at the nano-scale, the physics of nanoparticles mean that their properties are different from the properties of the bulk material.
This makes the size of particles or the scale of its features the most important attribute of nanoparticles." (An extract from http://www.malvern.co.uk/)

3.1.2. Peptide Nanoparticles

The novel type of nanoparticles, de-novo designed and being produced in our lab, mimicking the symmetry of polyhedral virus capsids (Figure 3.1), are meaningfully termed as Peptide Nanoparticles (specific design strategy will be discussed in a later section). In principle, formation of such a nanoparticle takes place *in-vivo* by the self-assembly of a single chain polypeptide comprised of two oligomerization motifs i.e. a pentameric and a trimeric coiled coils connected through a linker. Such a designed system allows formation of nanoparticles of 16 nm in diameter and 473 kD molecular mass [3]. Properly functionalized peptide nanoparticles could be suitable for drug-delivery, diagnosis and treatment of human diseases [4]. This could again be used as an efficient vaccination tool simply by attaching an antigen to the surface of the nanoparticles, leading to so-called "Repititive Antigen Display"[5].

3.1.3. Peptide Nanoparticles and Drug Delivery

A successful drug delivery vehicle should have the following characteristics: ability to accomplish controlled release of drugs, biocompatibility, bioavailability, limited toxicity and capacity of better targeting the specific tissues [6]. The drug delivery vehicles that are presently being used possess limitations due to toxicity and side effects, poor stability and suboptimal bioavailability due to short half-life in the blood stream [7]. The side effects of these drugs stem from poor targeting and hence, a high dose of administration. Therefore, a good drug delivery vehicle should

accomplish an effective cell targeting. Also, it has been observed that the particles with sizes less than 10 nm are rapidly excreted from the system. Hence a particle size of 10-100 nm is optimum for designing the new generation drug delivery system[8].

Nanoparticle-based drug delivery vehicles using biopolymers are thought to be the best. The sizes of the nanoparticles can be made so that they fall in the optimum size zone for an effective drug administration system. The ease of manipulation of such particles for controlled pharmacological needs is one of the valuable properties that could be utilized. Also, being biopolymer based, these systems are biodegradable.

The designed peptide nanoparticles in our lab would be of a diameter of ~20 nm. Owing to their biodegradability and cage like structure having a cavity of 6-10 nm diameter at the center (Figure3.6), they could be a useful mean for drug transport in the blood stream. The morphology, size, shape and targeting eficiency can be easily modified at the molecular level [9]. They can be used to deliver both small-molecule drugs and various classes of biomacromolecules, such as peptides, some inorganic compounds like gold, and quantum dots for use as a biosensor (to be discussed in detail later).

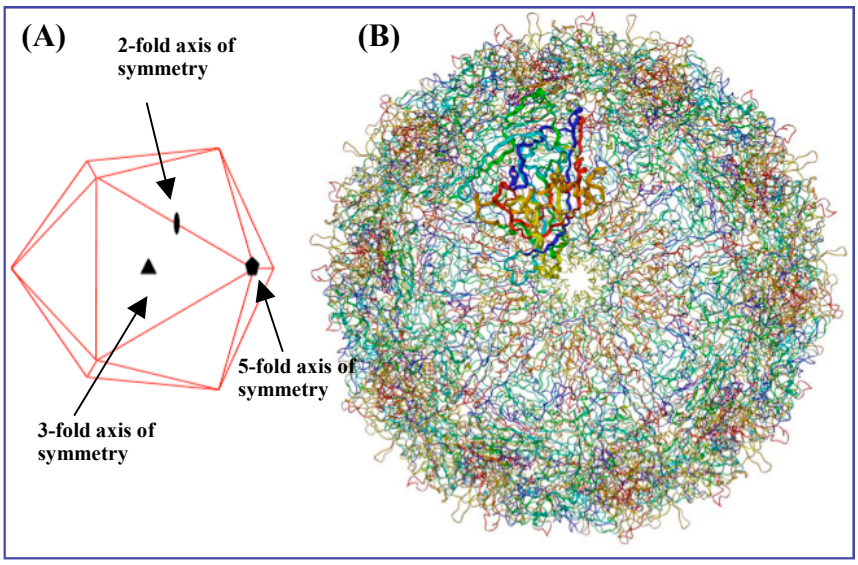

Figure3.1: Structure and geometry of icosahedral viral capsid.
A) Icosahedron elements with its symmetry
B) X-ray crystal structure (1DNV) of the insect parvovirus (Galleria mellonella denso-virus) with icosahedral symmetry. The protein chains are colored from red (N-terminus) to blue (C-terminus) and one single protein molecule is highlighted. The view is down the five-fold symmetry axis.

3.2.4. Peptide Nanoparticles and Vaccine Design

Peptide nanoparticles could also be designed as an effective tool for vaccination. Vaccination with peptide nanoparticles utilizes the concept of Repetitive Antigen Display (RAD). Nanoparticles, with an immunogenic peptide attached to it, can exhibit several copies of the same antigen on its surface, thus, elevating the levels of antigenic response a few fold more than a single copy of the antigen. Hence, the epitopes for deadly pathogens e.g. HIV (Human Immuno-deficiency Virus), SARS-Virus (Severe Acute Respiratory Syndrome Virus), pseudomona, can be easily engineered on the surface of such peptide nanoparticles with a view to elicit a high content of neutralizing antibody in the blood sera and generate a variety of different vaccines. One of the major advantages of such a vaccine candidate is, that it does not require the use of a live attenuated virus, although it mimicks the geometry and property of the RAD of a virus or virus-like particle (VLP). Therefore, the ease and flexibility of design excluding the use of living virus particles makes it an attractive strategy in the field of vaccine design.

3.2.4.1. Vaccine for HIV

According to the census report of 2006 39.5 million people are suffering from HIV infection among which 4.3 million are newly affected in the very year worldwide (http://data.unaids.org/pub/EpiReport/2006). Therefore, a vaccine to prevent HIV-1 infection or to reduce disease progression in infected individuals is an urgent public health requirement **[10]**. However, generation of an HIV vaccine is still a goal yet to achieve.

The understanding of the progression of the disease becomes easier when considering the structure of the virus gp41 protein of the HIV-1 envelope glycoprotein, which represents the core of fusion-active gp41[11, 12]. A probable mechanism of formation of a host-virus fusion complex is described in the Figure 3.2. Generation of an antibody against this fusion complex could inhibit the infection of HIV and hence this complex is a potent target for vaccine design. Visualization of the structure of gp41 could help identify a mean that resists the interactions between gp120 and the CD4+ coreceptor of the infecting cells[11]

3.2.4.2. What are gp41, gp120 and gp 160?

The HIV membrane has about 9-10 spikes of the glycoprotein (gp) called gp160 which are embedded and are generally involved in binding and membrane fusion of the virus particles to the host cell [13] (Figure 3.3). The two proteins gp41 and gp120

are two proteolytic products of gp160. Gp41 is membrane bound and gp120 resides in the membrane exposed part[14]. Gp120 is responsible for binding of the virus to its receptors and coreceptors. gp41 is comprised of an ectodomain, a transmembrane domain and a cytoplasmic domain. The extracellular domain mediates the fusion process (Figure 3.2). An N-terminal and a C-terminal heptad repeat motif (suggestive of coiled coil structure) of the ectodomain forms a fusogenic active 6-helix bundle structure (Figure 3.2) to facilitate the virus genome transfer to the host cell [15].

3.2.4.3. Vaccination Strategy:

The challenges to produce an HIV vaccine are as mentioned below:

a) CD4+ cells are the most important cells for the immune response to take place in the human system. These cells help form the secretory antibodies after interaction with the fragments of antigen bound B-cell. Hence, CD4+ cells thought to be giving the first line of defense in the human body against any foreign immunogen. HIV attacks on these very CD4+ cells by drastically diminishing immunoresponsiveness of the host cells

b) After infection, HIV undergoes mutations and recombinations inside the host cell to evolve into a new type of virus strain. So, to generate an antibody that will be effective for all the new clades are very difficult as it gives rise to enormous antigenic variation.

c) Most of the envelope proteins are heavily glycosylated making the antigenic epitopes inaccessible for antibody binding.

d) Lack of any animal model to test the efficacy of the designed vaccine.

Hence, the remedies to the above obstacles can be generated by the following means.

a) An antibody response should be made so that the fusion of the virus with the CD4+ cells is restrained. Hence, to design the vaccine the antigenic region should be chosen in such a way that it is located in the gp41/ gp120 envelope trimer that is responsible for the virus attachment.

b) The successful vaccine must be effective against a large number of different HIV variants (broad spectrum). It is a prerequisite to develop vaccines against a conserved region of the HIV epitopes, which are common to all the HIVs or, at-least, in most of the HIV subtypes.

A Repititive Antigen Display (RAD) system can resolve the problems of low titer antibody response. It has been seen that the highly ordered display of antigens, which is termed as RAD, on the surface of a virus or bacteria is effective in causing several fold higher immunogenic response.

d) An effective vaccine is likely to include components able to induce humoral and cellular immune response[16].

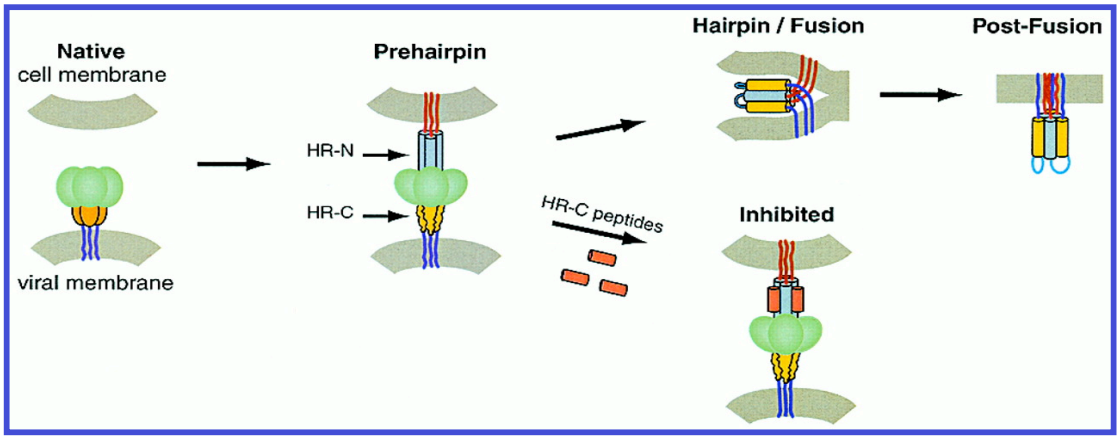

Figure 3.2. Working model of HIV-1 membrane fusion and its inhibition. Before exposure to cellular receptors, Env exists in a native state ("Native"). After interaction with CD4 and the coreceptor, a conformational change allows gp41, to form a transient prehairpin intermediate ("Prehairpin")[2]. (Figure is taken from the manuscript PNAS with a prior permission from Dr. Peter Kim).

In this thesis work, the HIV vaccine design was performed following the line of action as stated above.

a) **Choice of the epitope:** Elicitation of broadly neutralizing antibodies (i.e. antibodies those reduce or abolish the biological activity of the soluble antigen) against HIV-1 by immunization is a major challenge in developing a vaccine against the AIDS [17]. The immunogens that mimic the native structure of the gp41 ectodomain glycoprotein are found to form the most potent neutralizing antibodies. Only a few region of the envelope glycoprotein are actually accessible by the antibodies. A few human monoclonal antibodies, having the capacity to neutralize a broad range of primary isolates of HIV-1, have been isolated [18]. There are two monoclonal antibodies against the two vulnerable stretches of the transmembrane glycoprotein gp41 near the membrane proximal external region (MPER), namely, 2F5 and 4E10 [19, 20] (Figure 3.3). The MPER of gp41 is highly conserved, and several studies have implicated it as an essential part of the cell fusion machinery [21, 22]. For vaccine development, linear neutralizing epitopes have a potential advantage over more complex ones. Owing to the linear nature of the neutralizing epitopes it bears and to its high amino acid conservation, the MPER of gp41 is an attractive target for HIV-1 vaccine development. They have been found to be effective at a high concentration in protecting macaques from simian HIV challenge [23, 24]. 2F5 has been found to have a broad and potent neutralizing activity against primary HIV-1 isolates[25, 26]. A six-amino acid long peptide

sequence (ELDKWA) [27, 28] located near the C-terminus of the gp41 functions as the epitope and is well accessible by the antibody[29] [30]. Stiegler et. al.[31] reported that, 4E10 binds to a linear, highly conserved region of MPER (671-683) C-terminus to 2F5 epitope. Recent crystallographic structure determination has revealed the 4E10 epitope adopts a helical structure causing an effective structural constraint towards antibody production. The core peptide sequence of this epitope contains WF(D/N)IT [32]

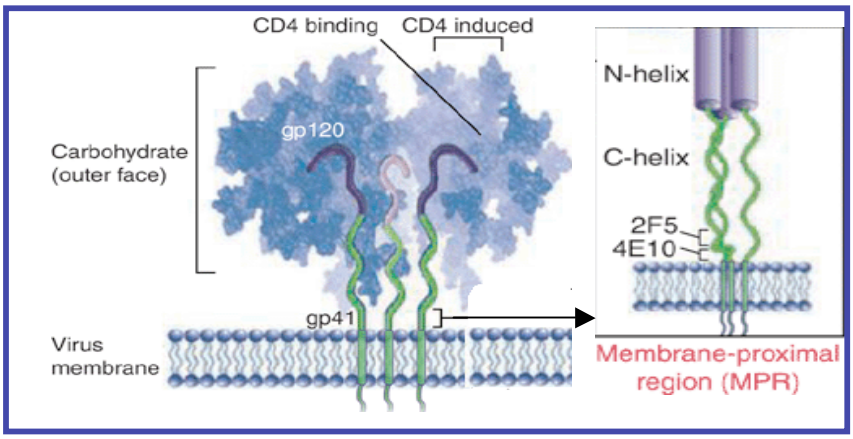

Figure3.3: Membrane proximal region of gp41 ectodomain in the HIV-1 virus membrane. The inset Figure clearly shows the location of the 2F5 and 4E10 antibodies binding sites. (Picture is taken form Nabel et al.[1]).

b) **RAD**: It is also desirable to elicit the antibody response in high titer in order to make an effective HIV-1 vaccine [17]. The immunogenic peptide (2F5-4E10) was attached to the peptide nanoparticle building block unit. 60 such monomeric units, upon self-assembly produce peptide nanoparticle with the HIV epitopes protruding out of the surface. Therefore, a single peptide nanoparticle unit is capable of displaying 60 antigenic peptides on its surface. This phenomenon of exhibiting multiple copies of the same epitope satisfies the concept of RAD.

c) **Generation of humoral immunity:** The antigenic 2F5-4E10 coupled epitope coupled to the peptide nanoparticle would be capable of eliciting strong humoral immune response.

These two broadly neutralizing antibodies (MAbs) 2F5 and 4E10, established by Katinger et. al. recognize linear epitopes whose core representative sequences ELDKWA (2F5) and NWF(d/N)IT (4E10), are located just before the TM (Trans Membrane) region (Figure 3.3). The whole stretch containing the 2F5 and 4E10 epitope has been selected to be the antigenic peptide to be exhibited on the peptide nanoparticle.

3.2.4.4. HIV-1 Vaccine Design

In this thesis, I report design of a nanoparticle with a peptide containing two of the HIV-1 epitopes, such that during the nanoparticle formation, the antigens for HIV-1 (a stretch of the gp41 containing the epitopes for 2F5 and 4E10) are displayed on the surface. This C-terminus HIV-1 epitope fusion with the nanoparticles could be used to achieve high titer antibodies by immunizing animals against HIV.

3.2.5. Nanoparticles and Biosensing

3.2.5.1. What is Biosensing?

"A biosensor is a device for the detection of an analyte that combines a biological component with a physicochemical detector component" [33]. A biosensor is composed of a sensing element, a sensitive biological element and a transducer. The sensing element identifies a particular species of interest through a specific reaction, absorption, or other physical or chemical process. The transducer maintains a connection between the other two elements and converts the results of this recognition into an electrical or optical signal that can be measured easily.

3.2.5.2. Peptide Nanoparticles in Biosensing

The thermo-optical properties of gold nanoparticles conjugated with the peptide nanoparticles expected to be a unique invention in the field of biomedicine. The coherent oscillation of the free electrons or the "surface plasmons" on the surface of the gold nanoparticles, is responsible for their unique optical absorption profile [34]. Surface plasmon resonance of the gold nanoparticles is sensitive to the change in the local environment/surface properties and results in a shift in the characteristic absorption spectrum. Hence, the optical properties of these particles are the function of geometry, shape and size and dielectric properties of the surrounding medium[35],[36]. Therefore, by controlling the dimensions and geometry, it is possible to manipulate the absorption and scattering wavelengths generated from gold nanoparticles. The above mentioned properties of gold nanoparticles had drawn attention in a wide variety of biomedical applications.

Gold and peptide nanoparticle composite can be made either by incorporating the gold nanoparticles in the core of the peptide nanoparticle or by decorating the peptide nanoparticle with the gold shell. These nanocomposites can be potentially used beacuse of their biocompatibility and biodebradability of the peptide unit. By adjusting the relative sizes and geometries of the core and the shell the optical

resonance of gold nanoshell can be manipulated in a very wide range; visible region to the infrared region [37] [38].

3.2.5.2.1. Cancer Therapy

An early detection of the metastases is the key challenge in the treatment of cancer. Until recently, there were no noninvasive method of detection and destruction of the cancer cells. Selective targeting of the cancer cell, leaving the healthy cells intact, is the major goal of modern cancer therapeutics[39]. Near IR radiation, coupled with metallic nanoparticles, confers an effective noninvasive technique in cancer detection and therapy. Such an IR radiation is chosen because of its nonionizability and tissue-penetrating capacity[40]. Flurophor or MRI contrast agent labelled metallic nanoparticles, after targeting to the diseased cells, when irradiated with near IR helps in visualizing metastases. The heat generated due to absorbtion of the incident radiation induces death of the affected cells. This is a very sophisticated improvement in the cancer therapeutics over the conventional surgical treatment in terms of precision and noninvasiveness. Moreover, in most cases, surgical therapy is unsuitable for early metastases and often affects the neighboring healthy tissues during the tratment process.

3.2.5.3. Gold Attached Peptide-Nanoparticle and Biosensing

Gold particles either can be layered on the nanoparticle surface making a gold nanoshell or incorporated inside the cavity of the peptide nanoparticle. The cancer cells generally have leaky membranes. Peptide nanoparticles bearing gold decorated in the surface diffuses well into the porous membrane of the cancer cells. The accumulated nanoparticles in the diseased cell upon illumination with near IR radiation would produce heat, which could help in visualization and photothermal destruction of the cells[41]. The gold nanoshells on the peptide nanoparticle scaffold are expected to have a broader range of wavelength absorption and scattering intensity, depending on the geometry of the composite structure and the thickness of gold making up the shell. The tunability of such particles make it a significant tool in the field of therapeutics. The tunability of these particles is exhibited by controlled variation of the core (peptide nanoparticles) and shell (gold nanoparticles) ratio (Figure 3.4).

In this thesis work for making gold and peptide nanoparticle composites, a peptide (e.g. A3 peptide[42]) that helps in seeding gold on its surface (constructs P3a_BB3) was attached to the peptide nanoparticle.

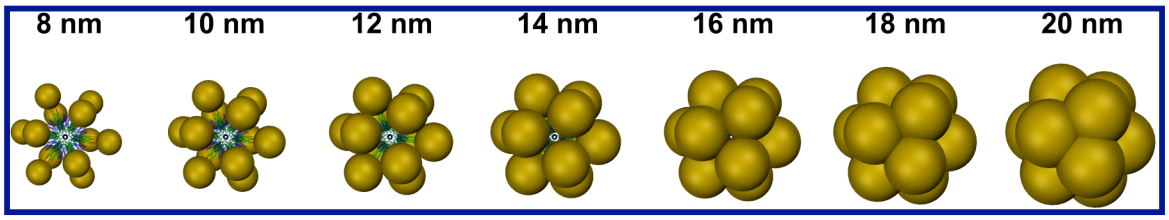

Figure 3.4. Depiction of the growing gold nanoparticles on the surface of the peptide nanoparticle. The diameter of the gold nanoparticles is indicated above. At a diameter of about 15 nm the gold nanoparticles start to aggregate and to form a gold shell around the peptide nanoparticle. The shell is already closed at 18 nm. The diameter of the whole complex of the rightmost particle is about 50 nm.

3.2.5.3.1. Objectives

The objective of this project is to generate a novel nanocomposite using peptide nanoparticle and gold nanoparticle, having unique spectroscopic properties. The peptide nanoparticle is used as a scaffolding device to conjugate surface modified gold nanoparticles.

3.2.5.4. Development of Peptide Nanoparticle Based Serodiagnosis Tools for *M.tuberculosis*

Tuberculosis or TB is *Mycobacterium tuberculosis* mediated airborne infectious disease, still remains as one of the deadliest in the world. Although, between the years 1985 and 1992 a considerable decrease in the number of cases in USA was observed, after this period, a threatening number of cases have been reported. This increment can be attributed to several factors, i.e.,

A) Appearance of Multi Drug Resistant (MDR) strains of Mycobacterium

B) Occurrence of Extensive Drug Resistant strain of *Mycobacterium Tuberculosis*, the so-called (XDR)

C) Incidences of HIV

Depending on the diseased states, TB could be of two types: Active and Dormant/ Latent. According to an estimate by the World Health Organization (WHO) in the year 2005, 8.8 million people worldwide reported to be infected with active tuberculosis and among them, nearly 1.6 million died[43]. Among these, over 90 % of the population constitute the cases from developing countries[44]. Active tuberculosis is the more fatal type of the two and develops the signs and symptoms of the disease, while, in the cases of latent tuberculosis the antibodies against the

bacteria form a layer surrounding the infection nuclei and resist the disease progression. However, in suppressed immune condition, i.e., HIV infected system or in condition where immunosuppressant drugs had been used, likelihood of developing tuberculosis is higher.

3.2.5.4.1. Clinical manifestation of Tuberculosis

Several factors determine the clinical manifestation of TB. The cumulative effect of all the factors results in remarkable variability in the disease progression. 75-85 % of the TB cases are found to be predominantly pulmonary[45]. Extra-pulmonary tuberculosis generally involves heart, kidney, lymph node, central nervous system, and genitourinary tract, etc. Extrapulmonary TB is more prevalent in children than adults. However, this proportion of pulmonary and extrapulmonary tuberculosis is quite different in the immuno-compromised system, e.g., in the HIV infected body[46]. Fever is the most common symptom of the disease, though there are many a cases where, at no point in the diseased stage, there was any fever. Loss of appetite, night sweatness, weight loss, weakness and malaises are other common signs of Tuberculosis. However, these symptoms are diagnostically difficult to pinpoint, as they are often confused with other diseases, if any, are coexisting. Extrapulmonary tuberculosis is the less frequent of the two types and less knowledge is available to the clinicians about it. Also, in these cases there is only limited access to the diseased organs, which again causes the trouble in detection of the disease.

3.2.5.4.2. Diagnosis of Tuberculosis

Generally one or more of the procedures as mentioned below are used in the diagnosis and determination of the efficacy of a given treatment of tuberculosis.

Diagnostic microbiology: Sputum test for Acid Fast Bacilli (AFB): Because mycobacterial infection can occur at almost any site of the body, a variety of samples from various sites could be submitted for the examination of the presence of the bacteria. The most common of the specimens is the sputum (mostly for pulmonary pathology), while the others include gastric filtrate, urine, cerebrospinal fluid etc.[47]. Following collection, the specimens are transported to the designated laboratories ASAP. The detection of the mycobacterium is routinely done by making a smear of the specimen and incubating it with an Acid Fast Dye, e.g., auramine (TB Fluorescent Stain Kit M; Difco Laboratories, Detroit, MI). This type of staining procedure is dependent on the dye-retaining capacity of the mycobacterium. The detection of the AFB in the stain is the first diagnostic evidence of the presence of mycobacteria[47]. However, a negative AFB test does not preclude the possibility of TB as optimum numbers of bacilli should be in the specimen for the successful detection ~ 5000-10000[48]. If the number is below that, it gives a false negative sputum test.

Tuberculin skin test: A positive Tuberculin Skin test is the indication of the latent tuberculosis[47]. This particular test is based on the fact that a few culture filtrates "purified protein derivatives"(PPD) or "Tuberculins" show delayed type of hypersensitivity in the patients who have been exposed to Mycobacterium. Tuberculin extract is injected below the skin in the forearm. A positive response is seen depending on the presence of active or latent TB in the patient after 24 -72 hr., showing a red swelling in the injected zone. Basically, this result is an example of the T-cell mediated response, where T-cells sensitized by prior infection accumulate in the injected tuberculin spot and secret lymphokines[49]. However, a tuberculin test cannot predict how long one has been exposed to the infection.

Chest X-ray: In the chest X-ray, there is a typical impression formed in the plate characteristics of tuberculosis infection. The appearance of several white areas in the dark background signifies such an infection[50]. However, sometimes the pulmonary lesions are not associated with positive radiograph images[51].

3.2.5.4.3. Difficulties in Diagnosis

The difficulties in diagnosis of tuberculosis stems from the fact that the disease is very slow progressing. Until it reaches a reasonably advanced stage, the symptoms of the disease are not so prominent.

The limitations of the diagnosis tools that are recently being used are multifold and are explained as follows.

a) Mostly, a negative sputum test outcome results in several visits of the patients and requires multiple samples and eventually the diagnosis is delayed[52]. The delay in identifying TB is responsible for 20 % of the TB transmission [53].

b) Microscopic examination is not sensitive, as it is dependent on the skill and mental condition of the micrscopist[44].

c) Symptoms of Extrapulmonary tuberculosis is nonspecific.

d) Granuloma culture and histological examination are not commonly available in the developing countries where the majority of the cases are being reported[54].

e) Due to the complexity and expensiveness in the invasive techniques it could not be practiced in the developing countries[52].

f) Present diagnosis methods are time consuming because of the slow growth rate of *M.tuberculosis*. This leads to high mortality rate.

Because of the above mentioned limitations, especially in the resourcefully challenged countries like India, Taiwan, Tanzania, it could be useful if any rapid and sensitive tuberculosis detection method could be employed. One such technique could be immunobased serodiagnostic system.

3.2.5.4.4. Serological Diagnostic System

The serological diagnostics assay relies on detection of antibodies in the serum of the respective patients. The previously developed serodiagnosis helps detecting, to some extent the pulmonary TB. However, to date, to our knowledge, there is no such detection system for extrapulmonary cases of the disease[54]. Also, a rapid diagnosis tool for paucibacillary TB is required immediately. The immune based system for the detection of tuberculosis has been unsuccessful for years. However, recently, the discovery of a few reactive antigens in the culture filtrate of *M.tuberculosis* that are recognized by the antibodies in the multibacillary and paucibacillary $HIV^{+}TB$ and $HIV^{-}TB$ patients, sounds promising in the diagnosis of pulmonary and extrapulmonary TB[55]. The two of these antigens are reported to be mycobacterium Malate synthase (MS) (an 81 kD enzyme) and MPT51 (a 27 kD protein) and these antigens are found to have their counteracting antibodies in $HIV^{-}TB^{+}$ patients (pulmonary) who are smear-positive from India[56]. Among the 60 smear positive TB patients studied in an experimental set up, 47 (78%) had anti-MS and 41(68%) had anti-MPT51 antibodies. Hence, 49 out of 60 patients (82 %) were shown to have either one or both of the antibodies as biomarkers in their sera[44]. The laboratory of Prof. Suman Laal at NYU, is constantly working on these antigens and already have shown experimental results which gives strong support for the effectiveness of these antigens as biomarkers in detecting incipient subclinical TB[44].

The advantages of the serodiagnostic tests are as follows:

1. They are cheap and easy to perform[54].
2. The specimen or the samples do not need to be from the site of infection[54]
3. Promptness in detection is one of the advantages of this type of technique that can be adapted for the so-called “point of care format”[54].
4. MS-MPT based serodiagnostic assays can very well serve for the detection of pulmonary TB as an adjunct to the sputum test[54].
5. This system is highly specific and sensitive in the detection of TB in a particular TB endemic region[44].
6. Performances of these particular biomarkers are not hampered due to the presence of HIV infection[44].

This MS_MPT based serodiagnostic system is capable of identifying sub-clinical TB[44].

Prof. Suman Laal in her laboratory at NYU has performed several tests in order to optimize a serodiagnostic tool. By the use of peptide mapping, they have found three different antigenic regions of the Malate sythase enzyme, which are mostly recognized by the antibodies in the sera of the TB patients at different stages and diseased conditions (data has not been published yet). Three regions of the Malate synthase enzyme sequence show the most immunogenicity, which correspond to the followings, i.e., 192-211, 237-258 and 620-630.

3.2.5.4.5. Peptide Nanoparticle in Serodiagnosis of Tuberculosis

The three peptides corresponding to the immunogenic regions of MS were designed to attach to the de-novo designed peptide nanoparticle constructs. Because of the size and RAD capacity, these nanoparticles will be able to expose multiple times on its surface and would have the ability to aggregate more strongly with the antibodies in the sera. Hence, the peptides attached to the nanoparticle would be more rapid and sensitive in terms of reaction to take place in the sera of the TB patients. In this thesis, I have tried to produce a single peptide nanoparticle on which all the three above-mentioned TB-antigenic peptide would be exhibited. Such a system with multiple malate synthase antigens displayed on the surface could be the most effective in showing the agglutination in the serodiagnostic assay settings. Here is a cartoon of what might happen in the blood serum of the TB infected patient when the nanoparticle based multiple antigen display system comprising of three antigens are exposed to the respective antibodies. The reaction mechanism that could take place leading to agglutination has been pictorially depicted in the Figure 3.5.

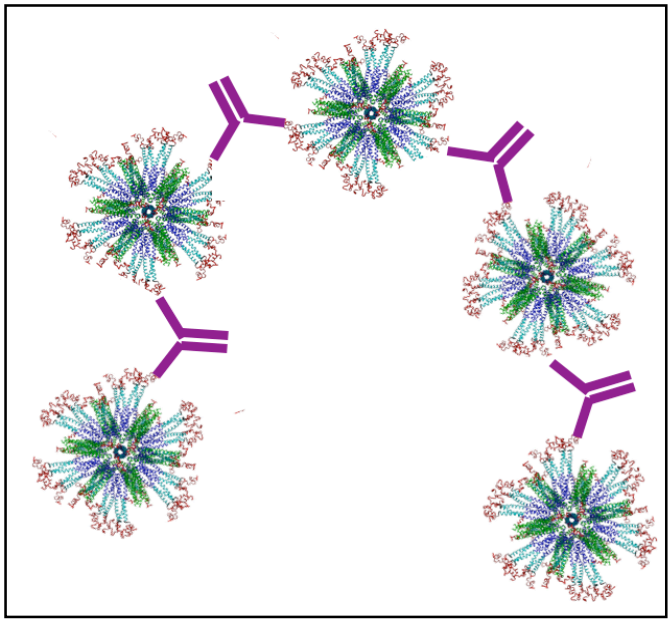

Figure 3.5: The agglutination of the antibodies in the presence of the antibodies. Antigens are the highly immunogenic parts of malate synthase attached on the surface of the peptide nanoparticle.

3.3. Objective of the Current Research

The primary aim of this thesis work is to produce a peptide nanoparticle. These nanoparticles were so designed to enable flexibility in addition/deletion/replacement of any sequence to the existing one with a view to improve the physical and chemical properties of them. One of the two constructs was so manipulated that it would produce a higher amount of protein than the other constructs being worked on in the lab. A higher yield would lessen the job of repeated protein extraction/purification provided the proper storage conditions for the produced nanoparticles are known. After successful formation, such peptide nanoparticles would be functionalized for various biomedical applications, e.g., designing HIV vaccine, producing serodiagnostic tools for Tuberculosis, gold seeding, making a gold nanoshell around the peptide scaffold. Along with the new construct the functional nanoparticles from the conventional construct (i.e., P3a) would be worked on and compared with the new one. Functionalized nanoparticles would be then characterized biophysically using CD spectroscopy, DLS, TEM etc. The efficency of vaccination of the HIV conjugated nanoparticle would be checked by immunzing the animal model (rat).